

## 广州塔闪电光谱特性分析

王雪娟<sup>1,2</sup>, 王海通<sup>1</sup>, 化乐彦<sup>1</sup>, 吕伟涛<sup>2\*</sup>, 陈绿文<sup>3</sup>, 马颖<sup>2</sup>, 齐奇<sup>2</sup>, 武斌<sup>2</sup>, 许伟群<sup>2</sup>, 杨静<sup>4</sup>, 张其林<sup>1</sup><sup>1</sup>南京信息工程大学气象灾害教育部重点实验室, 气候与环境变化国际合作联合实验室, 气象灾害预报预警与评估协同创新中心, 中国气象局气溶胶与云降水重点开放实验室, 江苏 南京 210044;<sup>2</sup>中国气象科学研究院灾害天气国家重点实验室, 北京 100081;<sup>3</sup>中国气象局广州热带海洋气象研究所, 广东 广州 510641;<sup>4</sup>中国科学院大气物理研究所, 中层大气和全球环境探测重点实验室, 北京 100029

**摘要** 利用广州高建筑物雷电观测站获得的 600 m 高广州塔上一次闪电 3 个回击放电过程的光谱资料, 详细分析了广州塔上闪电光谱随时间的演化和随高度的变化特性, 并通过对比实测的一组氮原子(NI)[856.8 nm, 859.4 nm, 862.9 nm]多重态的谱线强度比和理论计算值之比, 验证了闪电近红外光辐射满足光学薄条件。结果表明: 3 个回击放电通道约在 200 m 以下发光较强; 在回击放电初期, 当向上传输的电流波还未到达通道顶部时, 底部通道径向辐射光谱由较强的离子线和较弱的中性原子线组成, 而通道顶部径向辐射光谱主要取决于下行先导, 由较弱的离子线和较强的中性原子线组成; 当回击电流波向上传输到通道顶部后, 整个通道径向辐射出很强的离子线和很强的中性原子线, 且离子线总强度和原子线总强度均随通道高度的增加而减小; 在回击放电 70  $\mu$ s 以后, 200 m 以上通道离子线总强度和原子线总强度随通道高度的增加基本保持不变。此观测结果也直接证实了闪电放电通道由一个辐射离子线的高温核心和一个辐射中性原子线温度相对较低的外围电晕组成。

**关键词** 光谱学; 可见光谱; 近红外光谱; 广州塔闪电; 放电通道; 光学薄

**中图分类号** O433

**文献标志码** A

**DOI:** 10.3788/AOS221510

## 1 引言

近年来, 随着针对闪电放电过程物理特性研究的不断深入, 闪电等离子体的光谱诊断已成为测量闪电性质的重要工具。通过对光谱结构和演化的分析可以研究闪电发展微物理过程, 对光谱的定量分析也可以得到放电等离子体的基本物理特性参数<sup>[1-3]</sup>。最早, Orville<sup>[4-5]</sup>根据 10 m 长的自然云地闪电回击光谱资料对光谱的时间演化进行了初步分析, 并基于几条特定波长的谱线强度计算了通道温度。Warner 等<sup>[6]</sup>根据高速无狭缝摄谱仪观测的自然闪电梯级先导的光谱图像, 对 600~1050 nm 的先导红外光谱成分进行了分析。Xue 等<sup>[7]</sup>对两次自然云地闪电回击和 M 分量的光谱结构进行了分析, 并讨论了不同通道截面的光谱特征。Walker 等<sup>[8]</sup>报道了人工触发型闪电的高时间分辨光谱, 并分析了单、双电离的离子谱线以及中性原子线的时间演化特征。张华明等<sup>[9]</sup>对一次人工触发型闪电首次回击的发射光谱结构进行了分

析, 将闪电通道的导线部分与空气部分的发射光谱进行了比较。从以上分析可以看出, 目前对闪电光谱的观测研究主要是针对自然闪电和人工触发闪电两大类, 对高建筑物闪电的观测报道较少。由于高建筑物闪电相对于自然云地闪电发生的位置相对可预测, 发生的概率也相对较高, 且相对于人工触发闪电, 无需花费较大代价, 因此高建筑物可以为闪电研究提供良好的观测平台<sup>[10-12]</sup>。随着城市化的快速发展, 雷击高建筑物的概率越来越大。因此, 研究高建筑物闪电也可为高建筑物的雷电防护设计提供一定的实用参考。自 20 世纪 30 年代以来, 研究人员陆续开展了高建筑物闪电研究, 主要针对电磁特性和光学特征进行了观测和分析<sup>[6, 13-22]</sup>。目前国内外关于高建筑物闪电的光谱观测还鲜有报道。

通过闪电等离子体的光谱分析来测量闪电放电的物理参数, 就需要知道对于某一特定波长闪电通道的光学厚度<sup>[23]</sup>。根据等离子体对光吸收和散射的大小, 可将等离子体分为光学厚和光学薄等离子体。所谓的

收稿日期: 2022-07-21; 修回日期: 2022-08-29; 录用日期: 2022-10-26; 网络首发日期: 2022-11-04

基金项目: 国家重点研发计划(2017YFC1501504)、国家自然科学基金(42005065)、中国气象科学院灾害天气国家重点实验室开放课题(2020LASW-B14)、中国科学院中层大气和全球环境探测重点实验室(LAGEO)开放课题(LAGEO-2019-07)、南京信息工程大学大学生创新项目(XJDC202110300018)

通信作者: \*wtlu@ustc.edu

“光学薄”,就是辐射产生的光子在等离子体中传播时不会被吸收,能够全部发射出去;对于光学厚的等离子体,等离子体本身的自吸效应会对辐射出的谱线强度造成影响。Uman等<sup>[23]</sup>对利用测量的闪电可见波段光谱中的两个氮离子(NII)多重态谱线强度的比值与理论计算比值<sup>[24]</sup>及实验室测量比值<sup>[25]</sup>进行比较,结果表明闪电通道在可见波段的光辐射满足光学薄的定义。Wang等<sup>[26]</sup>通过对比实测的两组氮原子(NI)多重态的谱线强度比和理论计算值之比,实验上对闪电近红外光辐射的不透明度进行了验证。此外,由于以往的闪电光谱拍摄系统的光谱分辨率不足<sup>[27]</sup>和观测条件的限制,所获得的闪电光谱在红外波段具有共同上能级的多条谱线通常都处于无法分辨的谱线包络中。迄今为止,实验上关于闪电红外波段光谱中性原子线不透明度的验证还很少。

本文利用广州高建筑物雷电观测站(TOLOG)获得的600 m高广州塔上的闪电光谱资料,详细讨论了高建筑物广州塔闪电在放电过程中可见波段单电离的离子线和近红外波段中性原子线的时空演化特征;在此基础上,利用NI[856.8 nm, 859.4 nm, 862.9 nm]多重态对闪电在近红外波段光辐射是否满足光学薄条件进行了验证,所分析的闪电光谱特性具有一定的普遍意义。

## 2 基本原理

理论分析表明,在自旋-轨道耦合(LS耦合)条件下,通常相同高能级的多条谱线中只有一条谱线对不透明度敏感<sup>[28]</sup>。因此,可以通过谱线的强度比来讨论不透明度对闪电等离子体谱线强度的影响。如果等离子体满足光学薄,能级 $n$ 向能级 $r$ 跃迁发射的谱线强度可以表示为

$$I_{nr} = cN_n A_{nr} k\nu_{nr}, \quad (1)$$

式中: $I_{nr}$ 表示从能级 $n$ 向能级 $r$ 跃迁发射的谱线强度; $N_n$ 表示能级 $n$ 的原子数密度; $A_{nr}$ 表示爱因斯坦跃迁概率; $\nu_{nr}$ 表示发射光子的频率; $c$ 表示几何因子; $k$ 表示玻尔兹曼常数。

在局部热力学平衡(LTE)下离子辐射的能级按玻尔兹曼统计分布<sup>[29]</sup>,那么

$$N_n = \frac{Ng_n}{B(T)} \exp\left(-\frac{E_n}{kT}\right), \quad (2)$$

式中: $N$ 表示总的原子数密度; $E_n$ 表示能级 $n$ 的上激发能; $g_n$ 表示能级 $n$ 的统计权重; $T$ 表示电子温度; $B(T)$ 表示配分函数。将式(2)代入式(1),能级 $n$ 向能级 $r$ 跃迁发射的谱线强度可表示为

$$I_{nr} = c \frac{Ng_n}{B(T)} A_{nr} k\nu_{nr} \exp\left(-\frac{E_n}{kT}\right). \quad (3)$$

那么,同一原子(或离子)从光学薄的气体中辐射出的两条光谱线的理论强度比为

$$\frac{I_{nr}}{I_{mp}} = \frac{g_n A_{nr} \nu_{nr}}{g_m A_{mp} \nu_{mp}} \exp[(E_m - E_n)/kT]. \quad (4)$$

若两条谱线属于同一多重态,则上激发能和谱线频率几乎一样。那么在LTE条件下,同一多重态内的两条发射谱线的强度比可简化为

$$\frac{I_{nr}}{I_{mp}} = \frac{g_n A_{nr}}{g_m A_{mp}}. \quad (5)$$

Griem<sup>[24]</sup>、Uman<sup>[27]</sup>和Walker等<sup>[30]</sup>的研究表明,闪电通道内各粒子的准平衡时间、电子和离子动能的平衡时间均为 $10^{-8}$  s或更小的量级,所以闪电通道近似满足LTE条件,可以利用式(5)检验闪电通道光辐射的不透明度。

## 3 实验装置

本研究的实验资料来自TOLOG。自2009年以来,TOLOG利用各种先进的闪电探测设备对广州珠江新城高建筑物发生的闪电事件进行了综合观测<sup>[31-32]</sup>。2020年在TOLOG架设了无狭缝光栅光谱仪,其记录系统为高速摄像机(Photron FASTCAM Mini AX),光谱响应范围为400~1000 nm,感光度(ISO)为100000,一个像素的大小为 $20 \mu\text{m} \times 20 \mu\text{m}$ 。摄像机采用的镜头焦距为20 mm。摄谱仪的分光平面透射光栅刻线密度为600 lp/mm。本实验选取的光谱资料来自发生于广州最高建筑物——高度为600 m的广州塔顶部的一次闪电,此闪电包含3个回击。观测点与广州塔的距离约为3.3 km。高速摄像机的帧率设置为14400 frame/s,像素个数为 $870 \times 512$ ,每帧图像的曝光时间为67.7  $\mu\text{s}$ 。

## 4 结果与讨论

图1给出了此闪电3个回击放电过程的通道发光图片。为了方便表述,按回击发生的次序,将各回击标记为R1、R2、R3,并定义第一次回击(R1)发生时间为0 ms,闪电通道最底部高度(广州塔的塔尖)为0 m。图1中给出了各回击之前的一张先导图片。图1中3个回击之后都伴随有连续电流过程。连续电流是指雷暴云局部电荷中心在回击后沿原放电通道持续放电的过程,此时通道持续发光。由高速摄像资料可知,回击R1、R2和R3与其对应之后连续电流放电过程的通道发光持续时间分别约为3.82 ms、8.06 ms和3.96 ms。图1给出了各回击后放电过程前0.90 ms的图片。

图2(a)、(c)和(e)给出了对应于图1中闪电3个回击通道约337 m处的二维时间分辨光谱图。图2(b)、(d)和(f)分别为图2(a)、(c)和(e)中多重态NI[856.8 nm, 859.4 nm, 862.9 nm]的局部放大图。图3给出了3个回击放电通道约337 m处的三维时间演化光谱图。图3中的 $x$ 、 $y$ 、 $z$ 轴分别代表波长、时间和谱线相对强度。

在图2(a)和图3(a)中,回击R1放电0时刻,光谱



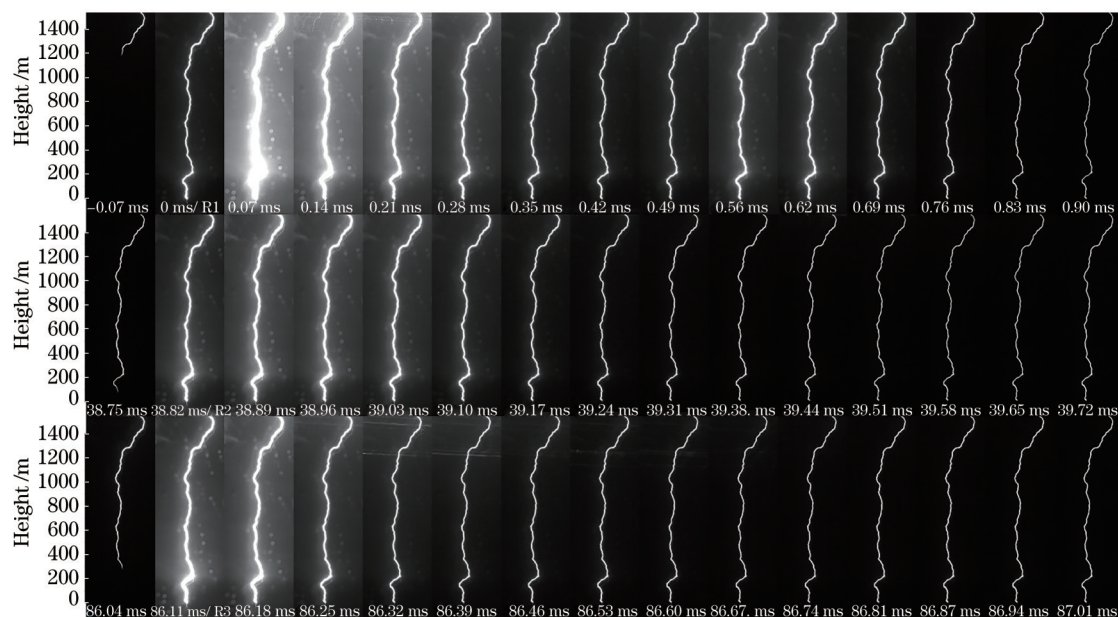


图1 闪电放电过程的高速摄像图片

Fig. 1 Original luminous images of the discharge process

在可见波段范围内(400~700 nm)能够很明显地观察到NII和H $\alpha$ 线,在红外波段(700 nm以上)也可以看到强度相对较弱的中性氮和氧原子(NI和OI)谱线。在第二帧0.07 ms,可见波段范围内的NII和H $\alpha$ 以及红外波段的NI和OI谱线强度都达到峰值。Orville<sup>[5]</sup>和Walker等<sup>[30]</sup>研究发现,闪电回击辐射光谱中最先出现离子线,当离子线强度低于阈值后,连续辐射和中性原子线再出现。但在图2(a)和图3(a)中,回击R1在0 ms,光谱中可见波段离子线刚出现时,通道已经辐射出中性原子线,在0.07 ms时,当可见波段离子线强度达到峰值时,中性原子线强度也明显较强。这显然与Orville<sup>[5]</sup>和Walker等<sup>[30]</sup>报道的观测结果不同。

比较辐射光谱中离子线与中性原子线的上激发能,可以发现,可见波段离子线的上激发能(20 eV以上)明显比红外波段中性原子线的上激发能(约10 eV)高。这说明在闪电通道径向方向有一个辐射离子线的高温区域和一个辐射中性原子线的相对低温区域。目前,已有研究中关于闪电通道的基本物理模型有两种:1)径向性质一致的通道<sup>[33-35]</sup>;2)由一个被低温电晕层包围的高温核心组成的通道<sup>[36-38]</sup>。本文的观测结果与第二种模型相符。Uman等<sup>[23]</sup>在1965年研究闪电可见波段离子辐射的不透明度时,理论分析表明,若闪电通道满足光学薄条件,闪电通道则由有效半径为毫米量级的高温核心和相对温度较低的外层电晕组成。他们指出,高温核主要含有单电离(也可能是双电离)离子,通道内的中性辐射由外层电晕的粒子密度和温度决定。本文为此结论提供了直接的实验观测证据。

从图2(c)、(e)和图3(b)、(c)可以看出,在回击R2和R3的第一帧,对应时刻为38.82 ms和86.11 ms,可

见波段的NII谱线强度已达到峰值。在第二帧,对应时间为38.89 ms和86.18 ms,可见波段的NII谱线强度急剧下降,H $\alpha$ 线及红外波段的NI和OI谱线强度达到峰值,之后H $\alpha$ 线及红外波段的中性原子线强度缓慢衰减。3个回击放电过程中,可见波段的离子线达到峰值后随时间均迅速减弱,而红外波段的中性原子线达到峰值之后随时间缓慢衰减。此外,从图2和图3可以看出,回击R1、R2和R3在放电初期(第一帧)可见波段离子线的发光强度明显强于近红外波段的中性原子线强度,但在放电后期,近红外波段的中性原子线明显强于可见波段的离子线。这与闪电在不同阶段产生辐射的物理机制有关。在回击的初始阶段(第一帧),放电通道核心内的原子被强大的回击峰值电流迅速电离,辐射出强烈的离子线。之后的连续电流过程中,通道内的回击电流缓慢下降,核心通道中的离子逐渐复合,并且通道径向发生能量传输,使整个通道辐射出中性原子线。

图4和图5给出了3个回击不同时刻的原始光谱图和沿通道变化的谱线图。图5中的 $x$ 、 $y$ 、 $z$ 轴分别代表波长、通道高度和谱线相对强度。图4(b)中恰好观测到通道底部电流传输时的光谱图。可以看到,回击R1在第一帧0 ms时,图4(b)中仅在通道底部辐射出较为明显的且激发能较高的离子线,通道顶部激发能较高的离子线较弱,而到图4(c)在0.07 ms时,整个通道从底部到顶部均辐射出较强的离子线。这表明图4(b)中放电高温核心通道的电流仅在通道底部传输,还未完全传输到通道顶部,而在图4(c)中,此时高温核心通道的电流已完全向上传输到通道顶部。因此,结合图4(b)和图5(a)可以得到,在回击电流波还未到达通道顶部时,通道底部径向辐射光谱由较强的离子线

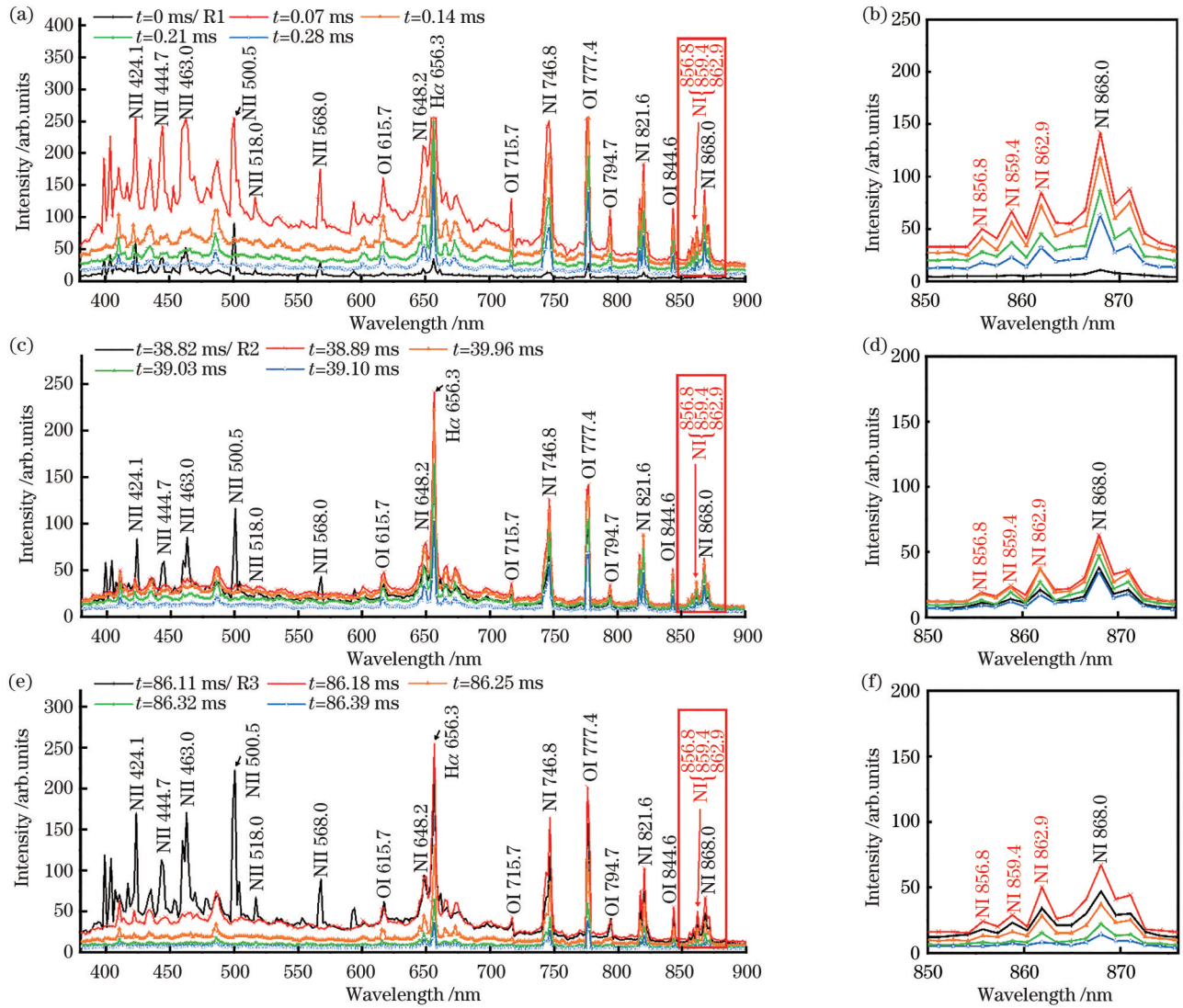


图2 3个回击通道高度约337 m处的二维时间分辨光谱以及多重态NI [856.8 nm, 859.4 nm, 862.9 nm]的局部放大图。(a) R1; (b) R1光谱中多重态NI [856.8 nm, 859.4 nm, 862.9 nm]的局部放大图;(c) R2;(d) R2光谱中多重态NI [856.8 nm, 859.4 nm, 862.9 nm]的局部放大图;(e) R3;(f) R3光谱中多重态NI [856.8 nm, 859.4 nm, 862.9 nm]的局部放大图

Fig. 2 Two-dimensional time-resolved spectrograms of three return strokes at channel height of about 337 m and magnified spectrograms of NI [856.8 nm, 859.4 nm, 862.9 nm] multiplet. (a) R1; (b) magnified spectrogram of NI [856.8 nm, 859.4 nm, 862.9 nm] multiplet for R1; (c) R2; (d) magnified spectrogram of NI [856.8 nm, 859.4 nm, 862.9 nm] multiplet for R2; (e) R3; (f) magnified spectrogram of NI [856.8 nm, 859.4 nm, 862.9 nm] multiplet for R3

和较弱的中性原子线组成,而通道顶部径向辐射光谱主要由较弱的离子线和较强的中性原子线组成。由于本实验拍摄得到的光谱为时间积分谱,当回击电流波还未到达通道顶部时,通道顶部的光辐射应该主要由前面下行先导决定。图4(c)和图5(b)中回击电流波完全向上传输到通道顶部后,此时整个通道径向辐射出很强的离子线和很强的中性原子线,但图5(b)、(c)中可见波段的离子线强度和红外波段的原子线强度随高度变化不大。观察图4(e)、(f),图4(h)、(i)和图5(d)~(g)中回击R2和R3第一帧38.82 ms、86.11 ms和第二帧38.89 ms、86.18 ms发现,通道内可见波段的离子线强度和红外波段的中性原子线强度随通道高度的变化趋势也不明显。研究表明,闪电光谱中的离

子线总强度与回击峰值电流正相关,光谱总强度与通道可视直径正相关<sup>[39-40]</sup>。离子线总强度和中性原子线总强度的变化可以分别反映通道核心电流和外围电晕电流<sup>[41]</sup>。为了进一步定量分析广州塔闪电放电过程中电流随通道高度的变化特征,图6给出了3个回击放电过程中通道光谱总强度、离子线总强度以及中性原子线总强度随高度的变化。

从图6可以看出,此闪电三次回击放电过程中光谱总强度(即通道发光总强度)均在通道底部200 m以下较强,超过通道高度200 m的位置,其光谱总强度减弱,并随高度的增加变化较为缓慢。但是个别高度如约620 m处,由图1和图4可知这一高度为通道发生弯曲的节点,在此节点处由于箍缩效应,对应通道高度光



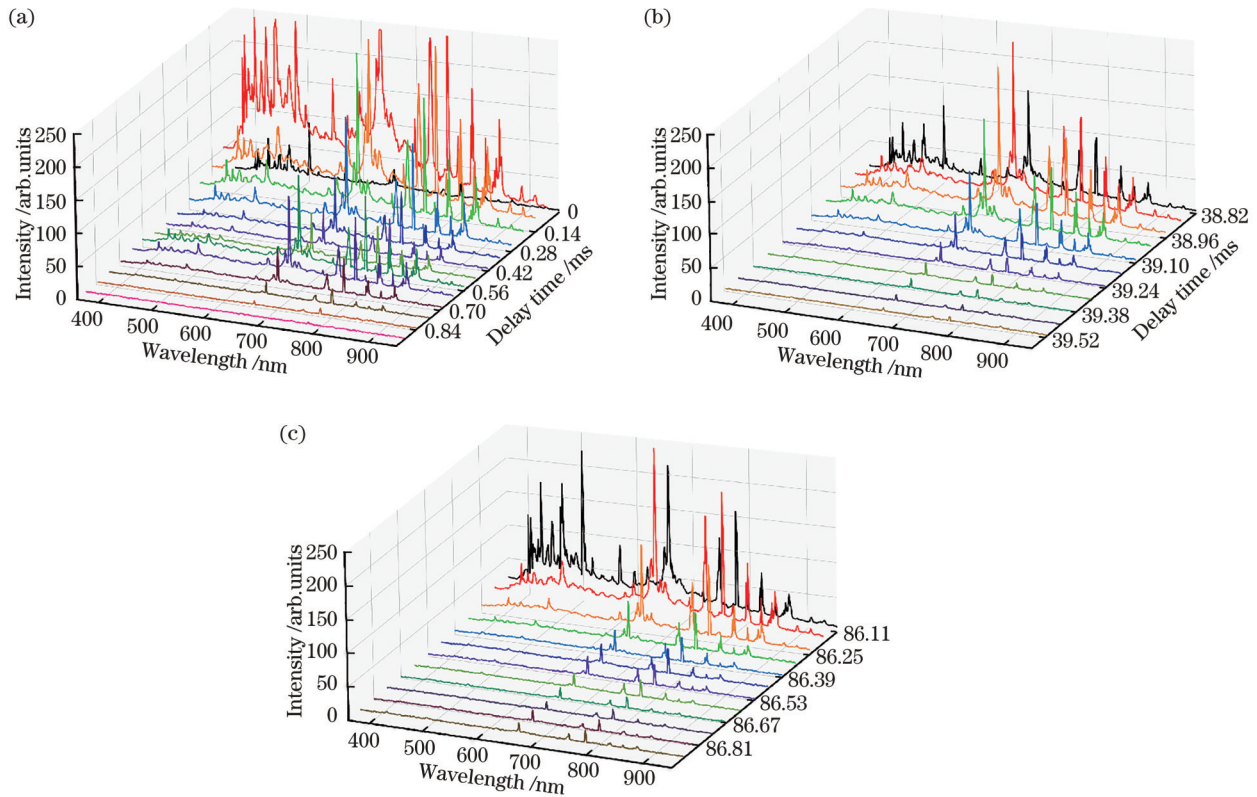


图 3 3 个回击在通道高度约 337 m 处的三维时间演化光谱。(a) R1; (b) R2; (c) R3

Fig. 3 Three-dimensional time evolution spectrograms of three return strokes at channel height of about 337 m. (a) R1; (b) R2; (c) R3

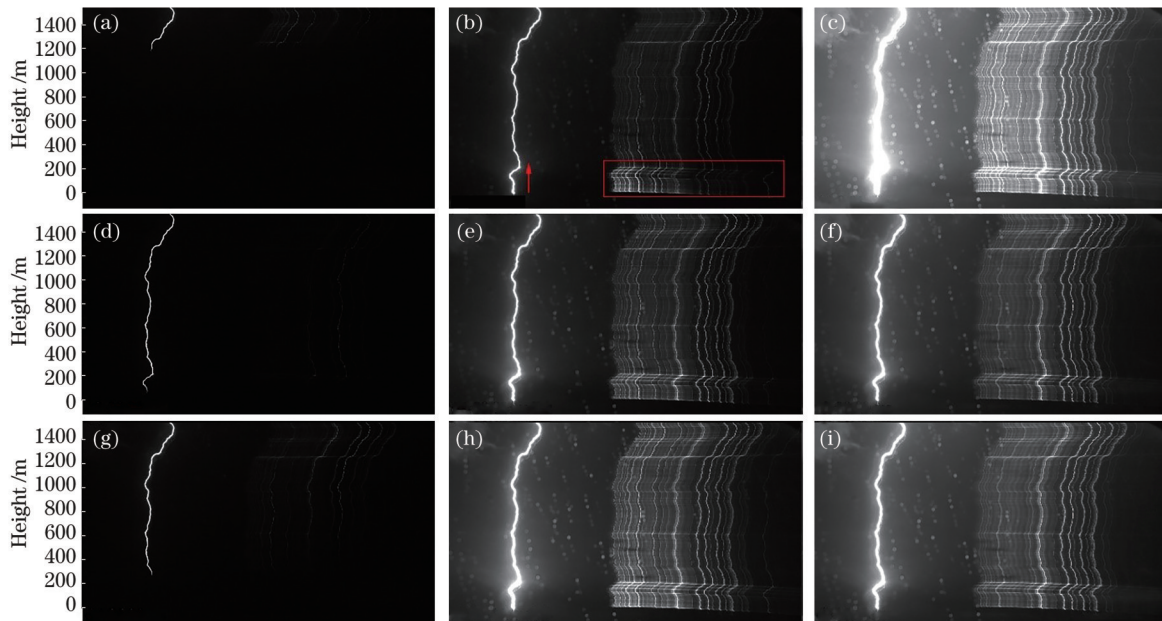


图 4 3 个回击的原始光谱。(a) R1, -0.07 ms; (b) R1, 0 ms; (c) R1, 0.07 ms; (d) R2, 38.75 ms; (e) R2, 38.82 ms;

(f) R2, 38.89 ms; (g) R3, 86.04 ms; (h) R3, 86.11 ms; (i) R3, 86.18 ms

Fig. 4 Original spectra of three return strokes. (a) R1, -0.07 ms; (b) R1, 0 ms; (c) R1, 0.07 ms; (d) R2, 38.75 ms; (e) R2, 38.82 ms;

(f) R2, 38.89 ms; (g) R3, 86.04 ms; (h) R3, 86.11 ms; (i) R3, 86.18 ms

谱总强度、离子线总强度和中性原子线总强度都出现增强。Tausanovic 等<sup>[42]</sup>报道当闪电击中地面时,放电过程土壤中的非线性会显著改变地面电阻,使闪电放电依赖于通道底部的电流。他们还指出,这也会产生

来自地面击中点的电流反射,强烈影响着放电通道,尤其是通道底部的电荷分布。因此,在闪电放电的击中点以上和以下的物理过程是相关的,不能独立地考虑。同时,放电通道底部的电流反射作用与通道底部电流

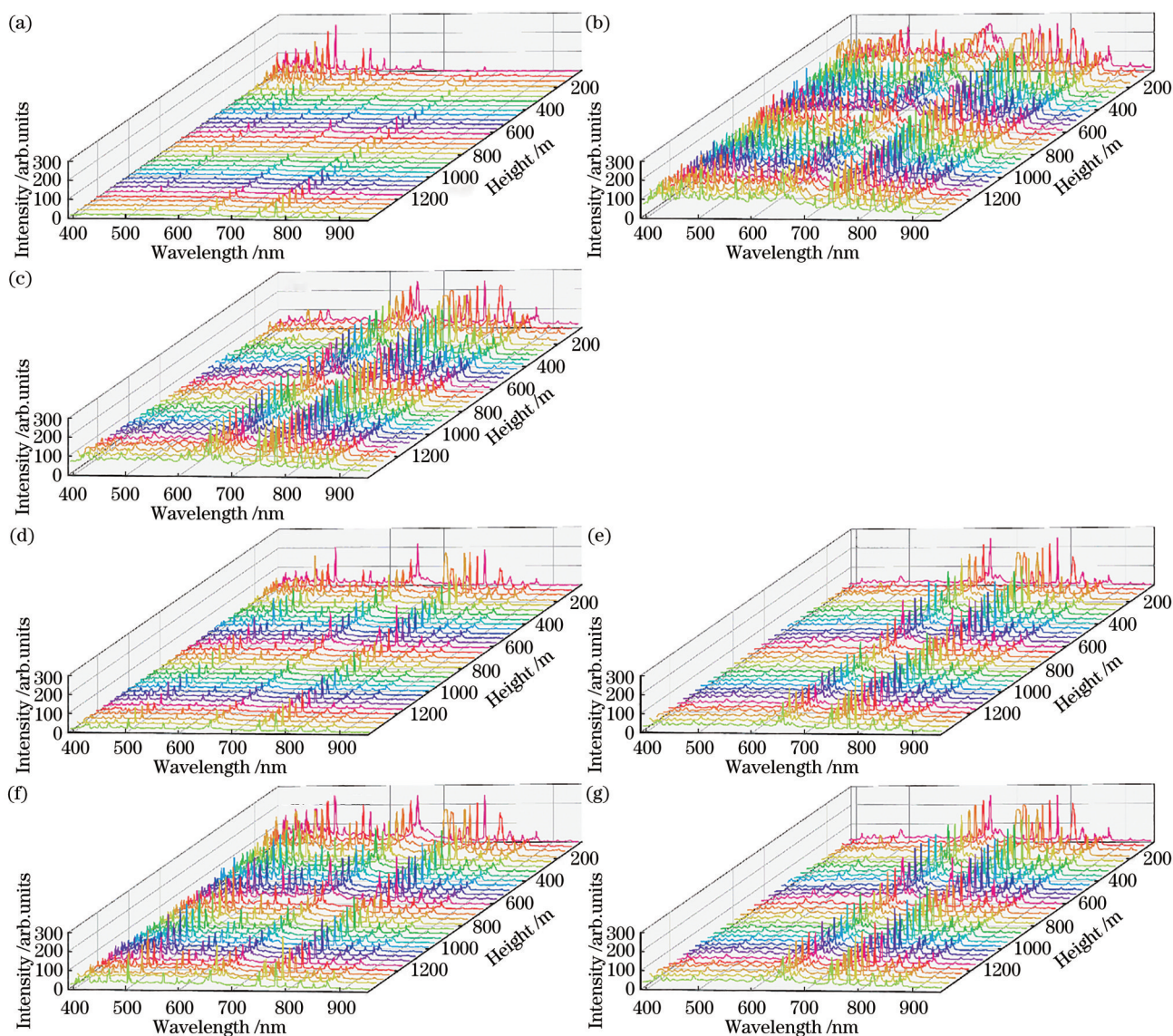


图 5 各回击在不同时刻沿通道高度变化的光谱图。(a) R1, 0 ms; (b) R1, 0.07 ms; (c) R1, 0.14 ms; (d) R2, 38.82 ms; (e) R2, 38.89 ms; (f) R3, 86.11 ms; (g) R3, 86.18 ms

Fig. 5 Variations of the spectrogram along the channel height for each return stroke. (a) R1, 0 ms; (b) R1, 0.07 ms; (c) R1, 0.14 ms; (d) R2, 38.82 ms; (e) R2, 38.89 ms; (f) R3, 86.11 ms; (g) R3, 86.18 ms

的大小也密切相关<sup>[43-45]</sup>。不同放电强度的闪电, 放电通道的电流反射作用也不同。图 6 中广州塔 3 个回击在放电过程中均在通道底部 200 m 以下有较强的光谱总强度, 这应该与建筑物底部和顶部的电流反射作用有关, 并且不同高度的建筑物上电流反射的作用范围应该也有所不同。关于高建筑物底部和顶部反射电流对闪电放电通道的影响, 这方面的报道目前非常少, 还需要进行深入的研究。

从图 6(a)可以看出, 回击 R1 第一帧 0 ms 放电初期, 离子线总强度在通道底部较高, 而中性原子线总强度在通道顶部较高。图 6(a)中原子线总强度在通道顶部较高, 其原因主要是受到先导的影响。由于摄像机拍摄的光谱为时间积分谱, 回击 R1 第一帧 0 ms 中通道顶部的原子线也包含先导向下发展时辐射的原子线。图 6(d)、(f)中, 对应回击 R2 和 R3 的第一帧

38.82 ms 和 86.11 ms, 离子线总强度和光谱总强度在通道底部也较高, 中性原子线总强度同样在通道底部较高。利用离子线总强度和中性原子线总强度分别反映放电通道核心电流和外围电晕电流。综上所述, 三次回击放电初期(第一帧), 通道核心的回击电流和外部电晕电流均随通道高度的增加呈减小趋势。图 6(e)、(g)中, 对应回击 R2 和 R3 的第二帧 38.89 ms 和 86.18 ms, 通道离子线总强度随高度变化不大, 光谱总强度和中性原子线总强度在通道高度 200 m 以上也变化不大, 这与回击 R1 在第二帧 0.07 ms 和第三帧 0.14 ms 时通道离子线总强度随通道高度的变化特征一致, 如图 6(b)、(c)所示。

由于自然云地闪电发生的时空随机性和观测条件以及环境的限制, 以往观测到的自然云地闪电光谱<sup>[39-41, 46]</sup>都无法很好地区分 NI [856.8 nm, 859.4 nm,



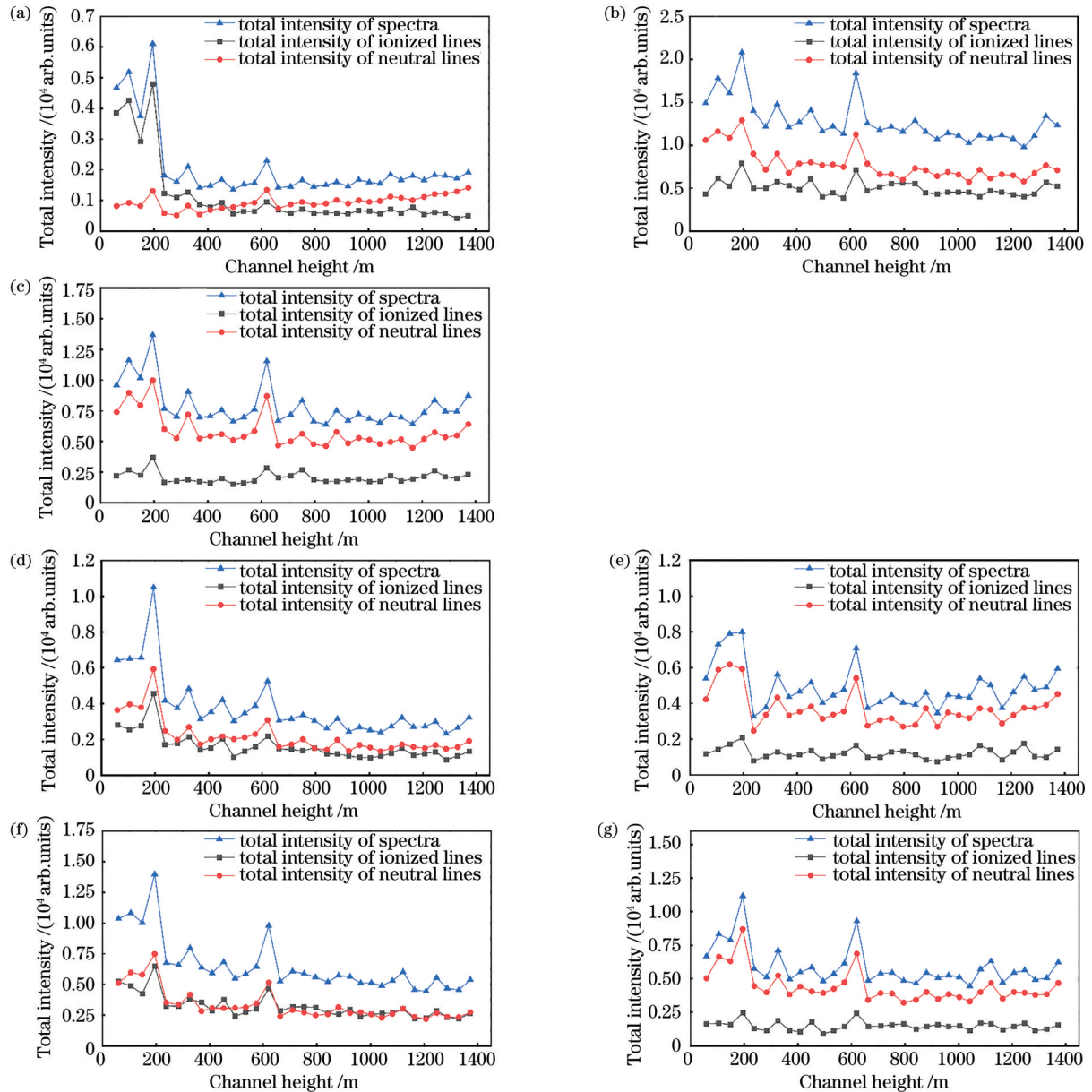


图6 各回击放电通道光谱总强度、离子线总强度以及中性原子线总强度随通道高度的变化。(a) R1, 0 ms; (b) R1, 0.07 ms; (c) R1, 0.14 ms; (d) R2, 38.82 ms; (e) R2, 38.89 ms; (f) R3, 86.11 ms; (g) R3, 86.18 ms

Fig. 6 Variations of total intensity of the spectra, total intensity of ionized lines, and total intensity of neutral lines along the channel height for each return stroke. (a) R1, 0 ms; (b) R1, 0.07 ms; (c) R1, 0.14 ms; (d) R2, 38.82 ms; (e) R2, 38.89 ms; (f) R3, 86.11 ms; (g) R3, 86.18 ms

862.9 nm]这一多重态。基于高建筑物闪电放电观测平台,本实验获取了分辨出多重态NI [856.8 nm, 859.4 nm, 862.9 nm]的高波长分辨率的光谱资料,如图2(b)、(d)、(f)所示。因此,通过式(5),可以进一步验证闪电通道红外波段辐射的光学特性。从图2(a)、(c)、(e)也可以看出,闪电近红外波段光辐射在整个放电过程均相对较强,且在这一波段,连续谱辐射相对较弱,分子散射也比可见波段弱<sup>[23]</sup>。因此,红外波段光谱是研究闪电不透明度的最佳选择。

在允许的误差范围内,如果实验测量的相同上激发能的两条谱线强度比与理论计算的 $gA$ (能级统计权

重与爱因斯坦跃迁概率的乘积)值比一致,可以认为闪电通道满足光学薄的条件。为了进一步验证闪电等离子体的近红外辐射满足光学薄条件,表1列出了由NIST数据库查询的各相关谱线的跃迁参数,图7给出了闪电光谱中NI [856.8 nm, 859.4 nm, 862.9 nm]多重态中谱线测量强度比与理论计算的 $gA$ 值之比。

理论计算得到NI 856.8/859.4 nm、856.8/862.9 nm和859.4/862.9 nm  $gA$ 值之比分别为0.46、0.18和0.91。由于式(5)给出的谱线强度比与通道温度或电子密度无关,那么多重态中谱线的强度比应该保持恒定不变。从图7可以明显看出,这一组多重态

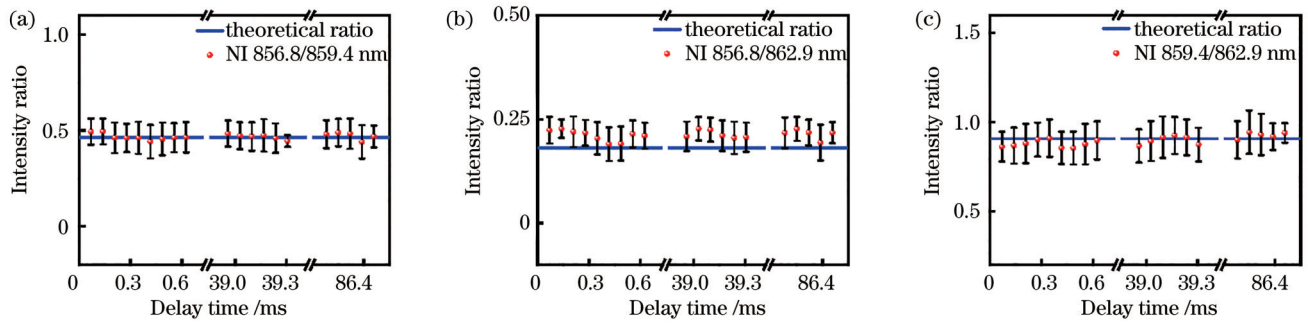


图 7 NI [856.8 nm, 859.4 nm, 862.9 nm]多重态测量谱线强度比和理论计算  $gA$  值之比。(a) NI 856.8/859.4 nm; (b) 856.8/862.9 nm; (c) 859.4/862.9 nm

Fig. 7 Intensity ratios of measured spectral lines and the ratios of theoretical  $gA$  values within the NI [856.8 nm, 859.4 nm, 862.9 nm] multiplet. (a) NI 856.8/859.4 nm; (b) 856.8/862.9 nm; (c) 859.4/862.9 nm

表 1 NI [856.8 nm, 859.4 nm, 862.9 nm]多重态的跃迁参数

Table 1 Transition parameters of NI [856.8 nm, 859.4 nm, 862.9 nm] multiplet

Wavelength /nm	Transition probability with statistical weight $gA / (\times 10^8 \text{ s}^{-1})$	Excitation energy $E / \text{eV}$	Upper level Conf., Term, J
856.8	0.194	12.126	$2s^2 2p^2(^3P) 3p^2 P_{3/2}^\circ$
859.4	0.418	12.122	$2s^2 2p^2(^3P) 3p^2 P_{1/2}^\circ$
862.9	1.07	12.126	$2s^2 2p^2(^3P) 3p^2 P_{3/2}^\circ$

内任意两条谱线测量强度比随时间基本保持不变,与理论预测结论一致。

从图 7(a)、(c)明显看出,NI 856.8/859.4 nm 和 859.4/862.9 nm 谱线的测量强度比与理论计算  $gA$  值之比符合得较好,但图 7(b)中 NI 856.8/862.9 nm 谱线的测量强度比误差相对较大。实验观测的谱线强度比有 3 个重要的误差来源:1)无法准确确定谱线轮廓的基底;2)不能准确分开这些多重态上叠加的其他 NI 谱线;3)叠加在所研究的这些 NI 多重态上的光谱噪声、无关谱线、连续谱等。其中第 3 个误差来源对实验结果的影响很明显。从图 2 可以看到,多重态 NI [856.8 nm, 859.4 nm, 862.9 nm]各谱线相比其他中性原子线强度较弱,而 NI 856.8/862.9 nm 的理论计算  $gA$  值之比相对较小,因此光谱背景噪声和连续谱对测量谱线强度的影响较大,导致图 7(b)中计算误差较大。除此之外,虽然表 1 中 856.8、859.4、862.9 nm 谱线的上激发能  $E$  值近似相等,但实际上它们不完全属于相同上能级的跃迁。跃迁 NI 859.4 nm 的上能级为  $2s^2 2p^2(^3P) 3p^2 P_{1/2}^\circ$ ,而跃迁 NI 856.8 nm 和 862.9 nm 的上能级为  $2s^2 2p^2(^3P) 3p^2 P_{3/2}^\circ$ ,它们是同一多重态但具有不同  $j$  值的能级,这也是引起图 7 中误差的原因。

一般情况下,实际测量谱线强度比与理论计算  $gA$  值之比的误差期望应在 10%~15%<sup>[23]</sup>。Uman 等<sup>[23]</sup>实际测得的两个氮离子(NII)多重态谱线强度比误差在 10%~30%。Wang 等<sup>[26]</sup>测得的 NI [742.4 nm, 744.2 nm, 746.8 nm]和 NI [818.8 nm, 821.6 nm, 824.2 nm]两个多重态的谱线强度比与理论计算  $gA$

值之比的平均误差为 8.37% 和 9.54%。本文中 NI [856.8 nm, 859.4 nm, 862.9 nm]多重态各谱线测量强度比与理论计算  $gA$  值之比的平均误差约为 15.65%。整体上,误差在合理范围内,且这些谱线的测量强度比变化稳定。上述结果表明闪电通道的近红外辐射光谱中 NI 线满足光学薄条件,所有测量的闪电通道内发生的中性辐射在等离子体中传播时不会被等离子体本身吸收,或者说自吸可以忽略。

## 5 结 论

基于 TOLOG 获得的一次广州塔上发生的三回击闪电光谱资料,对广州塔上闪电回击光谱随时空演化进行了分析,并通过对一组 NI 多重态各谱线的实测强度比与理论比的分析,实验验证了闪电近红外波段中性原子辐射满足光学薄条件。分析结果表明:3 个回击放电均在通道 200 m 以下发光较强。在回击放电初期,当电流波仅在通道底部传输,还未完全向上传输到通道顶部时,通道底部径向辐射光谱中可见波段离子线刚出现时,通道已辐射出较弱的中性原子线。当可见波段离子线强度达到峰值时,中性原子线强度也达到较强。这与以往报道的观测结果不同。此次观测结果直接证实了闪电通道内包含一个辐射离子线的高温核心和一个辐射中性原子线温度相对较低的电晕区域。并且在回击放电初期,离子线总强度和原子线总强度随通道高度增加而减小。在回击放电 70  $\mu\text{s}$  以后,通道 200 m 以上离子线总强度和原子线总强度随通道高度的增加基本保持不变。本研究一定程度上深化了对闪电放电微观物理过程的科学认识,也为闪电近红



外波段光谱的定量分析提供了实验数据。

### 参 考 文 献

- [1] 潘超超, 赵南京, 马明俊, 等. 基于激光诱导击穿光谱技术的土壤镉元素高灵敏检测研究[J/OL]. 激光与光电子学进展, 2022: 1-15[2022-07-17]. <https://kns.cnki.net/kcms/detail/31.1690.TN.20220714.1236.194.html>.  
Pan C C, Zhao N J, Ma M J, et al. Highly sensitive detection of Cd in soil based on laser-induced breakdown spectroscopy[J/OL]. Laser & Optoelectronics Progress, 2022: 1-15[2022-07-17]. <https://kns.cnki.net/kcms/detail/31.1690.TN.20220714.1236.194.html>.
- [2] 刘帅, 周木春. 基于火焰图像与光谱特征的炼钢终点温度预测[J/OL]. 激光与光电子学进展, 2022: 1-9[2022-07-16]. <https://kns.cnki.net/kcms/detail/31.1690.TN.20220713.1847.493.html>.  
Liu S, Zhou M C. Endpoint temperature prediction of converter steelmaking based on the characteristics of flame image and spectrum[J/OL]. Laser & Optoelectronics Progress, 2022: 1-9[2022-07-16]. <https://kns.cnki.net/kcms/detail/31.1690.TN.20220713.1847.493.html>.
- [3] 代玉银, 于丹, 李英华, 等. 不同空间约束壁数对激光诱导铜击穿光谱的影响[J]. 中国激光, 2022, 49(6): 0611001.  
Dai Y Y, Yu D, Li Y H, et al. Effect of different numbers of spatial confinement walls on laser-induced Cu plasma spectra[J]. Chinese Journal of Lasers, 2022, 49(6): 0611001.
- [4] Orville R E. A high-speed time-resolved spectroscopic study of the lightning return stroke: part I. A qualitative analysis[J]. Journal of the Atmospheric Sciences, 1968, 25(5): 827-838.
- [5] Orville R E. A high-speed time-resolved spectroscopic study of the lightning return stroke: part II. A quantitative analysis[J]. Journal of the Atmospheric Sciences, 1968, 25(5): 839-851.
- [6] Warner T A, Cummins K L, Orville R E. Upward lightning observations from towers in Rapid City, South Dakota and comparison with National Lightning Detection Network data, 2004-2010[J]. Journal of Geophysical Research: Atmospheres, 2012, 117(D19): 018346.
- [7] Xue S M, Yuan P, Cen J Y, et al. Spectral observations of a natural bipolar cloud-to-ground lightning: spectrum of bipolar CG lightning flash[J]. Journal of Geophysical Research Atmospheres, 2015, 120(5): 1972-1979.
- [8] Walker T D, Christian H J. Triggered lightning spectroscopy: part 1. A qualitative analysis[J]. Journal of Geophysical Research: Atmospheres, 2017, 122(15): 8000-8011.
- [9] 张华明, 张义军, 吕伟涛, 等. 一次人工触发闪电通道光谱结构分析[J]. 光谱学与光谱分析, 2017, 37(6): 1692-1695.  
Zhang H M, Zhang Y J, Lü W T, et al. The spectra structure characteristic of triggered lightning channel[J]. Spectroscopy and Spectral Analysis, 2017, 37(6): 1692-1695.
- [10] Janischewskyj W, Hussein A M, Shostak V, et al. Statistics of lightning strikes to the Toronto Canadian National Tower (1978-1995)[J]. IEEE Transactions on Power Delivery, 1997, 12(3): 1210-1221.
- [11] Hussein A M, Milewski M, Janischewskyj W, et al. Characteristics of lightning flashes striking the CN Tower below its tip[J]. Journal of Electrostatics, 2007, 65(5/6): 307-315.
- [12] Ishii M, Saito M, Natsuno D, et al. Lightning incidence on wind turbines in winter[C]//2014 International Conference on Lightning Protection (ICLP), October 11-18, 2014, Shanghai, China. New York: IEEE Press, 2014: 1734-1738.
- [13] Diendorfer G, Pichler H. Properties of lightning discharges to an instrumented tower and their implication on the location of those flashes by lightning location systems[C/OL]. 6th International Workshop on Physics of Lightning, 2006[2022-06-05]. <https://www.researchgate.net/publication/267725265>.
- [14] Kenneth L C, Krider E P, Mike O, et al. A case study of lightning attachment to flat ground showing multiple unconnected upward leaders[J]. Atmospheric Research, 2017, 202: 169-174.
- [15] Zhou H L, Diendorfer G, Thottappillil R, et al. Characteristics of upward positive lightning flashes initiated from the Gaisberg Tower[J]. Journal of Geophysical Research Atmospheres, 2012, 117(D6): 016903.
- [16] Jiang R B, Qie X S, Wu Z J, et al. Characteristics of upward lightning from a 325-m-tall meteorology tower[J]. Atmospheric Research, 2014, 149: 111-119.
- [17] Lü W T, Chen L W, Ma Y, et al. Lightning attachment process involving connection of the downward negative leader to the lateral surface of the upward connecting leader[J]. Geophysical Research Letters, 2013, 40(20): 5531-5535.
- [18] Wang Z C, Qie X S, Jiang R B, et al. High-speed video observation of stepwise propagation of a natural upward positive leader[J]. Journal of Geophysical Research: Atmospheres, 2016, 121(24): 14307-14315.
- [19] Yuan S F, Jiang R B, Qie X S, et al. Characteristics of upward lightning on the Beijing 325 m meteorology tower and corresponding thunderstorm conditions: upward lightning and thunderstorm[J]. Journal of Geophysical Research: Atmospheres, 2017, 122(2): 12093-12105.
- [20] Cummins K L, Krider E P, Olbinski M, et al. A case study of lightning attachment to flat ground showing multiple unconnected upward leaders[J]. Atmospheric Research, 2018, 202: 169-174.
- [21] Fan Y F, Lü W T, Lu G P, et al. Electromagnetic characteristics of upward leader initiated from the canton tower: a comparison with rocket-triggered lightning[J]. Journal of Geophysical Research: Atmospheres, 2021, 126(21): 034998.
- [22] Wu B, Lü W T, Qi Q, et al. A positive cloud-to-ground flash caused by a sequence of bidirectional leaders that served to form a ground-reaching branch of a pre-existing horizontal channel[J]. Journal of Geophysical Research: Atmospheres, 2021, 126(11): 033653.
- [23] Uman M A, Orville R E. The opacity of lightning[J]. Journal of Geophysical Research, 1965, 70(22): 5491-5497.
- [24] Griem H R. Plasma spectroscopy[M]. New York: McGraw-Hill, 1964.
- [25] Mastrup F, Wiese W. Experimentelle Bestimmung der Oszillatorenstärken einiger NII und OII Linien[M]. New York: Zeitschrift für Astrophysik, 1958, 44: 259-279.
- [26] Wang X J, Wang H T, Lü W T, et al. First experimental verification of opacity for the lightning near-infrared spectrum[J]. Geophysical Research Letters, 2022, 49(13): 098883.
- [27] Uman M A. Determination of lightning temperature[J]. Journal of Geophysical Research, 1969, 74(4): 949-957.
- [28] 张庆国, 贺健, 尤景汉. 不透明度对太阳日冕软 X 射线 OⅢ光谱线影响的研究[J]. 空间科学学报, 2014, 34(4): 384-389.  
Zhang Q G, He J, You J H. Research on the effect of opacity on solar coronal soft X-ray OⅢ spectral line[J]. Chinese Journal of Space Science, 2014, 34(4): 384-389.
- [29] 杨明磊, 刘玉柱. 基于激光诱导击穿光谱技术的条斑紫堇元素探测研究[J]. 激光与光电子学进展, 2022, 59(10): 1030001.  
Yang M L, Liu Y Z. Element detection in porphyra yezoensis via laser-induced breakdown spectroscopy[J]. Laser & Optoelectronics Progress, 2022, 59(10): 1030001.
- [30] Walker T D, Christian H J. Triggered lightning spectroscopy: 2. A quantitative analysis[J]. Journal of Geophysical Research: Atmospheres, 2019, 124(7): 3930-3942.
- [31] 吕伟涛, 陈绿文, 马颖, 等. 广州高建筑物雷电观测与研究 10 年进展[J]. 应用气象学报, 2020, 31(2): 129-145.  
Lü W T, Chen L W, Ma Y, et al. Advances of observation and study on tall-object lightning in Guangzhou over the last decade[J]. Journal of Applied Meteorological Science, 2020, 31(2): 129-145.

- [32] Lü W T, Chen L W, Zhang Y, et al. Characteristics of unconnected upward leaders initiated from tall structures observed in Guangzhou[J]. Journal of Geophysical Research: Atmospheres, 2012, 117(D19): 018035.
- [33] Schonland B F J. Progressive lightning IV-The discharge mechanism[J]. Proceedings of the Royal Society of London Series A: Mathematical and Physical Sciences, 1938, 164(916): 132-150.
- [34] Schonland B F J. The pilot streamer in lightning and the long spark[J]. Proceedings of the Royal Society of London Series A: Mathematical and Physical Sciences, 1953, 220(1140): 25-38.
- [35] Schonland B F J. The lightning discharge[M]//Encyclopedia of physics/handbuch der physik. Heidelberg: Springer, 1956, 22: 576-628.
- [36] Bruce C E R. The lightning and spark discharges[J]. Nature, 1941, 147(3739): 805-806.
- [37] Bruce C E R. The initiation of long electrical discharges[J]. Proceedings of the Royal Society of London Series A: Mathematical and Physical Sciences, 1944, 183(993): 228-242.
- [38] Orville R E. Spectrum of the lightning stepped leader[J]. Journal of Geophysical Research: Atmospheres, 1968, 73(22): 6999-7008.
- [39] Wang X J, Yuan P, Cen J Y, et al. Correlation between the spectral features and electric field changes for natural lightning return stroke followed by continuing current with m-components: spectra of cc and m-components[J]. Journal of Geophysical Research: Atmospheres, 2016, 121(14): 8615-8624.
- [40] Wang X J, Yuan P, Cen J Y, et al. Correlation between the spectral features and electric field changes of multiple return strokes in negative cloud-to-ground lightning[J]. Journal of Geophysical Research: Atmospheres, 2017, 122(9): 4993-5002.
- [41] An T T, Yuan P, Liu G R, et al. The radius and temperature distribution along radial direction of lightning plasma channel[J]. Physics of Plasmas, 2019, 26(1): 013506.
- [42] Tausanovic M, Ignjatovic M, Cvetic J, et al. Influence of current reflections from the ground on corona sheath dynamics during the return stroke[J]. Electric Power Systems Research, 2017, 143: 84-98.
- [43] Baba Y, Rakov V A. On the use of lumped sources in lightning return stroke models[J]. Journal of Geophysical Research: Atmospheres, 2005, 110(D3): D03101.
- [44] Baba Y, Rakov V A. Lightning electromagnetic environment in the presence of a tall grounded strike object[J]. Journal of Geophysical Research: Atmospheres, 2005, 110(D9): D09108.
- [45] Baba Y, Rakov V A. Lightning strikes to tall objects: currents inferred from far electromagnetic fields versus directly measured currents[J]. Geophysical Research Letters, 2007, 34(19): L19810.
- [46] An T T, Yuan P, Chen R R, et al. Evolution of discharge characteristics along the positive cloud-to-ground lightning channel[J]. Journal of Geophysical Research: Atmospheres, 2021, 126(5): 033478.

## Analysis on Lightning Spectral Characteristics of Canton Tower

Wang Xuejuan<sup>1,2</sup>, Wang Haitong<sup>1</sup>, Hua Leyan<sup>1</sup>, Lü Weitao<sup>2\*</sup>, Chen Lüwen<sup>3</sup>, Ma Ying<sup>2</sup>, Qi Qi<sup>2</sup>,  
Wu Bin<sup>2</sup>, Xu Weiqun<sup>2</sup>, Yang Jing<sup>4</sup>, Zhang Qilin<sup>1</sup>

<sup>1</sup>Key Laboratory of Meteorological Disaster, Ministry of Education (KLME)/International Laboratory on Climate and Environment Change (ILCEC)/Collaborative Innovation Center on Forecast and Evaluation of

Meteorological Disasters (CIC-FEMD)/Key Laboratory for Aerosol-Cloud-Precipitation of China Meteorological Administration, Nanjing University of Information Science & Technology, Nanjing 210044, Jiangsu, China;

<sup>2</sup>State Key Laboratory of Severe Weather, Chinese Academy of Meteorological Sciences, Beijing 100081, China;

<sup>3</sup>Guangzhou Institute of Tropical and Marine Meteorology, China Meteorological Administration, Guangzhou 510641, Guangdong, China;

<sup>4</sup>Key Laboratory of Middle Atmosphere and Global Environment Observation (LAGEO), Institute of Atmospheric Physics, Chinese Academy of Sciences, Beijing 100029, China

### Abstract

**Objective** The lightning locations of tall buildings are relatively predictable with high occurrence probability, and the lightning of tall buildings does not need a larger cost compared with artificially triggered lightning. Therefore, tall buildings can provide a good observation platform for lightning research. Additionally, with the rapid development of urbanization, the probability of lightning striking tall buildings is increasing. Thus, the study on the lightning of tall buildings can provide practical references for the lightning protection design of tall buildings. With deepening research on the physical characteristics of lightning discharge, the spectral diagnosis of lightning plasma has become an important tool for measuring lightning properties. At present, the observations and research of lightning spectra mainly focus on natural lightning and artificially triggered lightning, but there are few studies on lightning spectral observations of tall buildings. In addition, the optical thickness of the lightning channel is an important prerequisite for quantitative analysis of the lightning spectrum. Due to the lack of spectral resolution in previous experimental systems, the experimental verification of the optical thickness of lightning NI and OI radiation in the near-infrared spectrum is rare. This paper employs the spectra of one lightning with three return strokes on the 600-meter-high Canton Tower obtained at the Tall Object Lightning Observatory in Guangzhou (TOLOG) to analyze the evolution and variation characteristics of the spectra with the time and



the channel height in detail. Experimental verification of the optical thickness of lightning near-infrared radiation is also presented by comparing the measured intensities of spectral lines of NI [856.8 nm, 859.4 nm, 862.9 nm] multiplet with the theoretical values. This study hopes to deepen the scientific understanding of the microcosmic physical process of lightning discharge and provide an experimental basis for the quantitative analysis of the near-infrared lightning spectrum.

**Methods** The TOLOG with six stations is established by Chinese Academy of Meteorological Sciences and Guangdong Meteorological Service. Spectral observations are set up at Station 1 and recorded by a slitless spectrograph with a high-speed camera. The splitting system of the spectrograph is a plane transmission grating, which is placed tightly in front of the objective lens of the camera. Based on the spectra of one lightning with three return strokes on the 600-meter-high Canton Tower, the evolution and variation characteristics of the spectra with the time and the channel height are analyzed. In addition, the influence of opacity on the spectral line intensity of lightning plasma can be determined with the intensity ratio of the spectral lines, and one way to determine the optical thickness is to compare the intensities of several lines with the same upper energy level within the same multiplet. Thus, after comparing the measured intensities of spectral lines of NI [856.8 nm, 859.4 nm, 862.9 nm] multiplet with the theoretical values, this study presents the experimental verification of the optical thickness of lightning near-infrared radiation.

**Results and Discussions** The results show that the discharge channels of three return strokes on the Canton Tower have stronger luminescence below 200 m (Fig. 6). In the initial discharge stage of the return stroke, when the upward current wave does not reach the top of the channel, the radial spectral radiation at the bottom of the channel is composed of stronger ionized lines and weaker neutral lines. Meanwhile, the radial spectral radiation at the top of the channel mainly depends on the downward leader and is composed of weaker ionized lines and stronger neutral lines (Figs. 4–5). When the current wave is transmitted to the top of the channel, the whole channel radially radiates strong ionized lines and strong neutral lines, and the total intensities of ionized lines and neutral lines all decrease with the increasing channel height (Figs. 4–5). After 70  $\mu$ s discharge, the total intensities of ionized lines and neutral lines remain basically unchanged with the channel height above 200 m (Figs. 5–6). This observation directly confirms that the lightning channel consists of a hot core radiating ionized lines and a cold peripheral corona radiating neutral lines. Additionally, intensity ratios of the spectral lines and the theoretical optically thin limit within the NI [856.8 nm, 859.4 nm, 862.9 nm] multiplet show that the measured ratios of NI lines within this multiplet are basically unchanged with the time (Fig. 7), which means that the near-infrared spectrum of the lightning channel meets the optically thin condition.

**Conclusions** Based on the spectra of one lightning with three return strokes on the 600-meter-high Canton Tower obtained at the TOLOG, the evolution and variation characteristics of the spectra with the time and the channel height are analyzed first in detail. Experimental verification of the optical thickness of lightning near-infrared radiation is also presented by comparing the measured intensities of spectral lines of NI [856.8 nm, 859.4 nm, 862.9 nm] multiplet with the theoretical values. The results show that the discharge channels of three return strokes on the Canton Tower have stronger luminescence below 200 m. In the initial discharge stage of the return stroke, when the upward current wave does not reach the top of the channel, weak neutral lines in the near-infrared band are radiated by the channel when the ionized lines in the visible band just appear in spectrum at the bottom of the channel. When the intensity of ionized lines in the visible band peaks, the intensity of neutral lines in the near-infrared band also peaks. This is different from previously reported observations, which directly confirms that the lightning channel consists of a hot core radiating ionized lines and a cold peripheral corona radiating neutral lines. In the initial discharge stage of the return stroke, the total intensities of ionized lines and neutral lines all decrease with the increase in the channel height. After 70  $\mu$ s discharge, the total intensities of ionized lines and neutral lines remain basically unchanged with the channel height above 200 m.

**Key words** spectroscopy; visible spectrum; near-infrared spectrum; Canton Tower lightning; discharge channel; optically thin